J. Crop Prot. 2022, 11 (2): 287-300

Research Article

Into the interference between *Beet curly top Iran virus* and *Beet curly top virus*: *in silico* evaluation of the role of the interaction between Rep and the nonanucleotide motif

Saeid Tabein* **and Seyed Ali Hemmati**

Department of Plant Protection, Faculty of Agriculture, Shahid Chamran University of Ahvaz, Ahvaz, Iran.

Abstract: *Beet curly top Iran virus* (BCTIV) and *Beet curly top virus* (BCTV) are responsible for the curly top disease in sugar beet *Beta vulgaris* L. and many other plants. Mixed infection by BCTIV and BCTV in sugar beet plants results in a synergistic interaction, with more severe symptoms than plants infected by either virus, accompanied by an increase in BCTIV and a decrease in BCTV titers. Interaction of the Replication associated protein (Rep) with the nonanucleotide motif within the origin of replication is crucial for the replication of the geminivirus genome. Using an *in silico* approach, we investigated the possible contribution of the interaction between Rep and the nonanucleotide motifs in the interference between BCTIV and BCTV in mixed infections. The physicochemical characterization of both Reps was performed, and their secondary and tertiary structures were predicted by SOMPA tool and I-TASSER server, respectively. Then, the binding affinity of each Rep towards cognate and non-cognate viral nonanucleotide motifs was assessed using Docking simulations. Cluster analysis of HADDOCK revealed that the total binding energy of BCTV Rep toward its cognate nonanucleotide motif was lower than for the BCTIV complex, confirming a higher affinity of BCTV encoded Rep for its nonanucleotide motif. Interestingly, the BCTIV Rep showed the highest affinity for the nonanucleotide motif of the non-cognate BCTV nonanucleotide motif. Since the replication of geminiviruses relies on species-specific Rep interactions and activities, this result could be considered responsible for the competitive interference of BCTIV towards BCTV.

Keywords: IBCTVs, mixed infections, nonanucleotide motifs, Rep, docking simulation

Introduction

Curly top is a widespread and destructive disease in several crops, weeds, and ornamental plants in Iran. It is identified by a range of symptoms, including vein enation, leaf curling, severe stunting, and significant crop losses (Anabestani *et al*., 2016). Two members of the *Geminiviridae* family, *Beet curly top Iran virus* (BCTIV), belonging to the *Becurtovirus* genus and *Beet curly top virus* (BCTV), belonging to the *Curtovirus* genus, are the causal agents of curly

Handling Editor: Masoud Shams-bakhsh

* Corresponding author: s.tabein@scu.ac.ir
Received: 18 April 2022, Accepted: 01 September 2022
Published online: 26 September 2022

[DOR: 20.1001.1.22519041.2022.11.2.10.3]

top disease in sugar beets (*Beta vulgaris* L.) and some other dicot plants in Iran (Anabestani *et al*., 2016; Gharouni Kardani *et al*., 2013).

Being geminiviruses, BCTIV and BCTV have a monopartite circular genome of single-stranded DNA encapsidated within twinned icosahedral particles (Zerbini *et al*., 2017). Despite similar biological characteristics, such as natural transmission by *Circulifer haematoceps* (family *Cicadellidae*) (Taheri *et al*., 2012) and seed transmission in a local variety of petunia (Anabestani *et al*., 2017), these Iranian beet curly top viruses (IBCTVs) have distinct genomic properties (Heydarnejad *et al*., 2013; Soleimani *et al*., 2013). BCTIV, the first described member of the genus *Becurtovirus*, shows an unusual genome organization and a novel nonanucleotide sequence ‘‘TAAGATTCC’’ within the origin of replication (*Ori*), with two nucleotide substitutions at positions 4 and 8 (Varsani *et al*., 2014) compared to the highly conserved ‘‘TAATATTAC’’ motif found in the majority of geminiviruses, including curtoviruses. The genome organization of curtoviruses includes seven open reading frames (ORFs), separated by a single intergenic region (IR). In contrast, the genome of becurtoviruses comprises two ORFs on the virion-sense strand and three on the complementary-sense strand, separated by a small (SIR) and a large (LIR) intergenic regions (Varsani *et al*., 2014; Bolok Yazdi *et al*., 2008). Interestingly, while the virion sense units of becurtoviruses and curtoviruses are similar, the complementary sense units are organized differently. In fact, the C1 and C2 ORFs of becurtoviruses are identical to the corresponding ORFs of geminiviruses belonging to the genus *Mastrevirus* and, contrary to curtoviruses, lack the C3 and C4 ORFs (Bolok Yazdi *et al*., 2008). Finally, as in mastreviruses, the Rep of becurtoviruses is expressed from a spliced transcript and contains an intron sequence (Bozorgi *et al*., 2017), while that of BCTV is encoded only by the C1 ORF (Varsani *et al*., 2014). Rep is the only geminiviral protein required for viral replication that occurs through a rolling-circle-replication (RCR) mechanism (Behjatnia *et al*., 1998). It has been proven that the interaction between Rep and the nonanucleotide motif within the intergenic region is fundamental for replication (Jeske *et al*., 2001).

Mixed infections of plant viruses are common in nature. Several important virus diseases of plants result from interactions between causative agents, generally categorized as synergistic or antagonistic (Syller, 2012). Synergistic interactions between BCTIV and BCTV were reported in sugar beet plants, resulting in more severe symptoms in sugar beet plants compared to plants infected by individual viruses. However, while BCTV induces more severe symptoms in some of its host plants, including sugar beet, during mixed infection BCTIV DNA titer increased at the expense of BCTV (Majidi *et al*., 2017).

The structure of Rep proteins and/or their interactions with the nonanucleotide motifs could be critical factors responsible for the competition between BCTIV and BCTV in mixed infection. Therefore, in the present study, we predicted the structures of the Rep proteins of the two curly top viral agents and estimated their interactions with the respective and non-cognate nonanucleotide motifs by computational analysis based on docking simulation.

Materials and Methods

Analysis of amino acid sequences of Rep proteins

The reference genome sequences of BCTIV (accession number JQ707939) and BCTV (accession number X97203.1) and the deduced amino acid sequences of Rep were obtained from the GenBank database of NCBI. The Rep of BCTIV is encoded by a spliced messenger RNA from C1 and C2 ORFs. The continuous sequence of C1: C2 ORFs of BCTIV (nucleotides 1482-2710) was considered to deduce the complete Rep sequence by eliminating the 155 nt introns (nt 1890-2044) from the spliced messenger RNA encoding the

[DOR: 20.1001.1.22519041.2022.11.2.10.3]

Rep of BCTIV (Bozorgi *et al*., 2017). Therefore, the full sequence encoding the Rep of BCTIV (1482-2710 nt position), without the intron, was considered in modeling studies of the Rep protein structure. In the case of BCTV, the C1 ORF (nt 1775-2836) was used to predict the structural model of Rep. Similarity index of the sequences with other known Rep sequences retrieved from GenBank database was estimated using the NCBI BlastP server (Altschul *et al*., 1997). Amino acid sequence alignment of the Reps of BCTIV and BCTV was carried out by CLUSTAL W (Thompson *et al*., 1994). The Expasy ProtParam server was further used for the physicochemical characterization (molecular weight, theoretical isoelectric points (pI), instability index, aliphatic index, and a total number of negatively (Asp+Glu) and positively charged residues (Arg+Lys)) of the proteins (https://web.expasy.org/protparam/). The SOPMA (Self-Optimized Prediction Method with Alignment) tool (http://npsa-pbil.ibcp.fr /cgi-bin/npsa_automat.pl?page=npsa_sopma.html) was used to predict the secondary structure of the IBCTVs encoded Rep proteins. Next, the transmembrane segments were identified using the TMHMM server (http://www.cbs.dtu.dk /services/TMHMM).

Homology modeling of Rep proteins of IBCTVs

To predict the structural models of the Rep proteins of IBCTVs, the selected genomic sequences of BCTIV and BCTV were analyzed by Iterative Threading ASSEmbly Refinement server (I-TASSER) (Zhang, 2008), checking the quality of the structures based on their C-score, TM-score and RMSD. The confidence score (C-score) estimates the models' global accuracy, while the TM-score assesses the topological similarity of the protein structures. RMSD is also a quantitative measure of structural similarity between two or more protein structures (Pawlowski *et al*., 2008). According to previous reports, the RMSD score between 1 and 2 Å represents closely related proteins, while TM-score between 0.5 and 1.0 indicates the superimposed proteins may have a similar fold. Moreover, the C-score strongly correlates with the quality of the final models and is typically in the range of -5 to 2, while higher C-score values represent a model with high confidence.

Moreover, the reliability of the predicted models of the two Rep proteins was assessed by Ramachandran plot, Verify-3D score, WHAT-IF packing quality scores (https://servicesn. mbi.ucla.edu/SAVES/) and PROSA energy/Z-score (https://prosa.services.came.sbg.ac.at/ prosa.php). PROCHECK compares the geometry of the residues in the models with stereochemical parameters derived from the high-resolution X-ray structures by Ramachandran plot analysis. VERIFY_3D checks the local environment of each residue in the modal, which is measured by a 3D profile, including the statistical preferences for the relative burial of residues, the fraction of side-chain area, and the local secondary structure (Colovos and Yeates, 1993). ERRAT analyzes the statistics of atom-atom contacts between different atom types (nitrogen, carbon, and oxygen), used for differentiating between correctly and incorrectly determined regions of protein structures, and a score above 50 is generally acceptable. It corresponds to a high-quality model (Al-Khayyat and Al-Dabbagh, 2016). In the PROSA web tool, the Z-score of a protein is determined as the deviation of the total energy between the native fold of the structure and the energy distribution resulting from random conformations. A Z-score outside a range characteristic for native proteins indicates erroneous structure. Finally, the packing quality of the residues of the structure was investigated by WHAT-IF server, where values above -5 indicate reliable models. Furthermore, the structural models of proteins were refined using $3D^{refine}$ web server (http://sysbio.rnet.missouri. edu/3Drefine/).

Docking analysis

Docking analysis was performed between the Reps of IBCTVs and their nonanucleotide

[DOR: 20.1001.1.22519041.2022.11.2.10.3]

motifs using the HADDOCK (High Ambiguity Driven protein-protein Docking) web server (de Vries *et al*., 2010; Kurkcouglu *et al*., 2018), using the best model obtained from I-TASSER. With HADDOCK, the plausible residues contributing to the protein-nucleotide interface are either active, defined as the residues that make contact within the complex, or passive, known as the residues that potentially make contact. Firstly, all residues of Rep were defined as passive. Moreover, all residues in the nonanucleotide motifs were considered active residues, and passive residues were automatically determined by default in the program. The HADDOCK protocol consisted of 1000 rigid-body docking solutions followed by a semi-flexible refinement of the 200 best complex models in explicit water. Using the HADDOCK default settings, conclusive selected structures were clustered based on RMSD criteria ranked on the basis of averaged HADDOCK score. Superimposed view of the binding complex between Reps and the nonanucleotide motifs in HADDOCK was obtained by the CHIMERA software (version 1.14) (Pettersen *et al*., 2004). Schematic view of the hydrogen bond interactions and nonbonded contacts between the nonanucleotide and the residues involved in the Rep binding site was provided by the PDBsum server (de Beer *et al*., 2014).

Results

Sequence analysis of Rep proteins

The full-length sequence of BCTIV-Rep gene consisted of a 1071 nt fragment (GC content 59.8%) encoding a 357 amino acids (aa) polypeptide with a calculated molecular weight of 41.86 kDa and pI of 6.83, an aliphatic index of 72.63, and an instability index of 54.73. The BCTV-encoded Rep gene (1059 nt, GC content 60.7%) encodes a protein of 353 aa with an approximate molecular weight of 40.2 kDa, a pI of 6.83, an aliphatic index of 76.60, and an instability index of 36.77 (Table 1).

The amino acid sequence alignment obtained with the UniProt database indicated that BCTIV Rep shares only 30% similarity and 23% identity with BCTV Rep (Fig. 1).

Prediction of secondary and tertiary structures of IBCTVs encoded Rep proteins

The analysis of the secondary structure of Reps predicted by the SOPMA tool indicated that both proteins contain random coils as the predominant component among the secondary structure elements (49.58% and 45.61% for BCTIV and BCTV, respectively), followed by α-helix (29.41% and 33.14% for BCTIV and BCTV, respectively), and β-sheet (16.53% and 16.43% for BCTIV and BCTV, respectively) (Table 1; Fig. 2).

Table 1 Summary of primary structure analysis and secondary structure prediction for Rep proteins of BCTIV and BCTV.

Tool	Parameters	BCTIV	BCTV
ProtParam	Number of amino acids	357.00	353.00
	Molecular weight (Da)	41866.44	40207.28
	Theoretical isoelectric point (pI) [a]	6.83	6.83
	Total number of negatively charged residues (Asp + Glu)	43.00	40.00
	Total number of positively charged residues (Arg + Lys)	42.00	39.00
	Instability index	54.73	36.77
	Aliphatic index	72.63	76.60
	GRAVY[b]	- 0.584	-0.58
SOPMA	α-helix (%)	29.41	33.14
	Extended strand (β-sheet) (%)	16.53	16.43
	β-turn (%)	4.48	4.82
	Random coil (%)	49.58	45.61

[a] The value of the overall net surface charge of a protein molecule.
[b] Grand Average of Hydropathicity index.

[DOR: 20.1001.1.22519041.2022.11.2.10.3]

```
CLUSTAL O(1.2.4) multiple sequence alignment

BCTIV MPRAPNRNRPTPNQPGYLRFQKKNAFLTYSQIGGDFKDYIFEKLKTLLESYVILFLAVSL 60
BCTV  -------------MPF--YKKAKNFFLTYPQCSVTKEDAL-EQLLAINTPSNKKYIRIC- 43
                     *     : ** **** * .   :* : *:* ::       :: :.

BCTIV EHHQPTEEQPEGGFHTHCIIQCDKKLDVNGNLFFNIILP-DGRTIHPRIDGLNAPKRAFE 119
BCTV  -----RELHDNGEPHLHALIQFEGKVQIRNARYFDLQHRSTSKQFHCNIQGAKSSSDVKS 98
            * : :*  * *.:** : *::::..  :*::     .: :* .*:* :: . . .

BCTIV YITKEDTSPRTFGELRLGGRSPNSIGNSNVEW-RRILDSSNTKEEFFSNIRESCPTDFVL 178
BCTV  YVSK-DGDHIDWGEFQVDGRSARGGQQTANDAAAEALNA-GNALEALQIIREKLPEKYIF 156
      *::* * .   :**:::.*** ..  ::  :   . *:: ..  * :. ***. * .:::

BCTIV RWPSILSFANYHFRPVVQPYTPR--WTEFSRLPDTIKEWAEQNIYFEPDNRPVRPRSLYI 236
BCTV  QYHNLKPNLEAIFLPPPDLFQPPFPLSSFTRVPDIIQEWADSYFGLDP-AAPFRYNSIII 215
      :: .:    :  * *  : : *    :.*:*:** *:***:. : ::*   *.* .*: *

BCTIV CGPSRTGKTQWARSLGRHHYMSGMVLDWSLYDIDHTTYHIIDDIRYQKIQQELFKSIIGC 296
BCTV  EGDSRTGKTMWARCLGPHNYITGHLDFSLKTYSDNVLYNVIDDVDPNYLKMKHWKHLIGA 275
       * ****** ***.** *:*::* :        *:. *::***:  : :: : :* :**.

BCTIV NEDYSVWIKHKPNLVIPGGRPCIAITNPDMDWI------PCMSESMKDWFYANCDVYYLA 350
BCTV  QREWQTNLKYGKPRVIKGGIPSIILCNPGEGSSYQDFLNKSENEALRSWTLQNSVFAKLT 335
      :.::.. :*:    ** ** *.* : **. .         . .*:::.*   *. .  *:

BCTIV SDEVWYS------------ 357
BCTV  S-PLFDNNQEASSQDQTSL 353
      *  :: .
```

Figure 1 Multiple sequence alignment of the amino acid sequences of the replication associated proteins of BCTIV (accession number: JQ707939) and BCTV (accession number: X97203.1) by CLUSTAL W software. Spliced mRNA of C1:C2 ORFs was translated to produce the Rep protein sequence of BCTIV, here compared to the BCTV Rep.

A

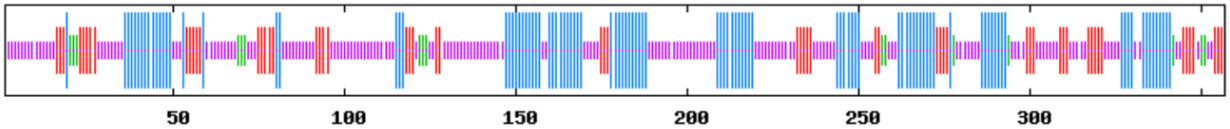

B

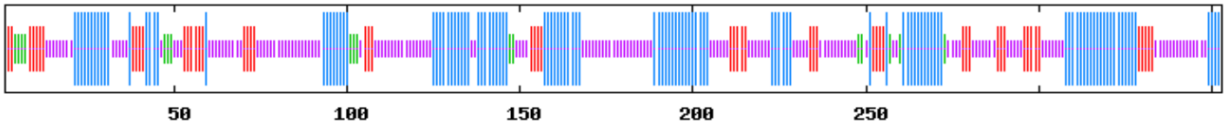

Figure 2 Comparison of the secondary structure of Rep proteins from BCTIV (**A**) and BCTV (**B**). Amino acids were identified using colors available as default in the SOPMA program (blue: α-helix, red: β-sheet, green: β-turn, purple: random coil).

[DOR: 20.1001.1.22519041.2022.11.2.10.3]

Table 2 Quality score of the predicted models of Rep proteins from BCTIV and BCTV with quality control software.

Parameters	BCTIV	BCTV
C-score	-3.25	-2.25
TM-score	0.35	0.45
RMSD	14.50	11.90
PROCHECK (%)	49.80	60.00
VERIFY_3D (%)	76.47	66.86
ERRAT (%)	58.16	63.34
Z-score	-3.61	-3.87

Here, the model with a lower RMSD and TM-score and a lower value of C-score were considered the confident models. Besides, results showed that 49.80% and 60% of the Rep residues were placed in the most favored regions for BCTIV and BCTV, respectively (Table 2, Fig. 3C, D). VERIFY_3D indicated that over 75% and 65% of residues of the Rep models for BCTIV and BCTV, respectively, have a score between 0.2 and 0.71, and can therefore be considered acceptable (Fig. 3E). The ERRAT scores were about 58.16% and 68.34% for BCTIV and BCTV, respectively (Table 2), showing that the overall quality of nonbonded interactions in the protein structures was appropriate. The Z-scores of both models were calculated to be about -3.61 and -3.87 for BCTIV and BCTV, respectively, similar to the values commonly found in the native structure of proteins (Table 2). Finally, the packing quality of each residue by WHAT-IF showed that all the scores for each residue were above zero. Overall, these results confirmed that the predicted models are reliable; therefore, the best-fitted models were considered for further docking analysis.

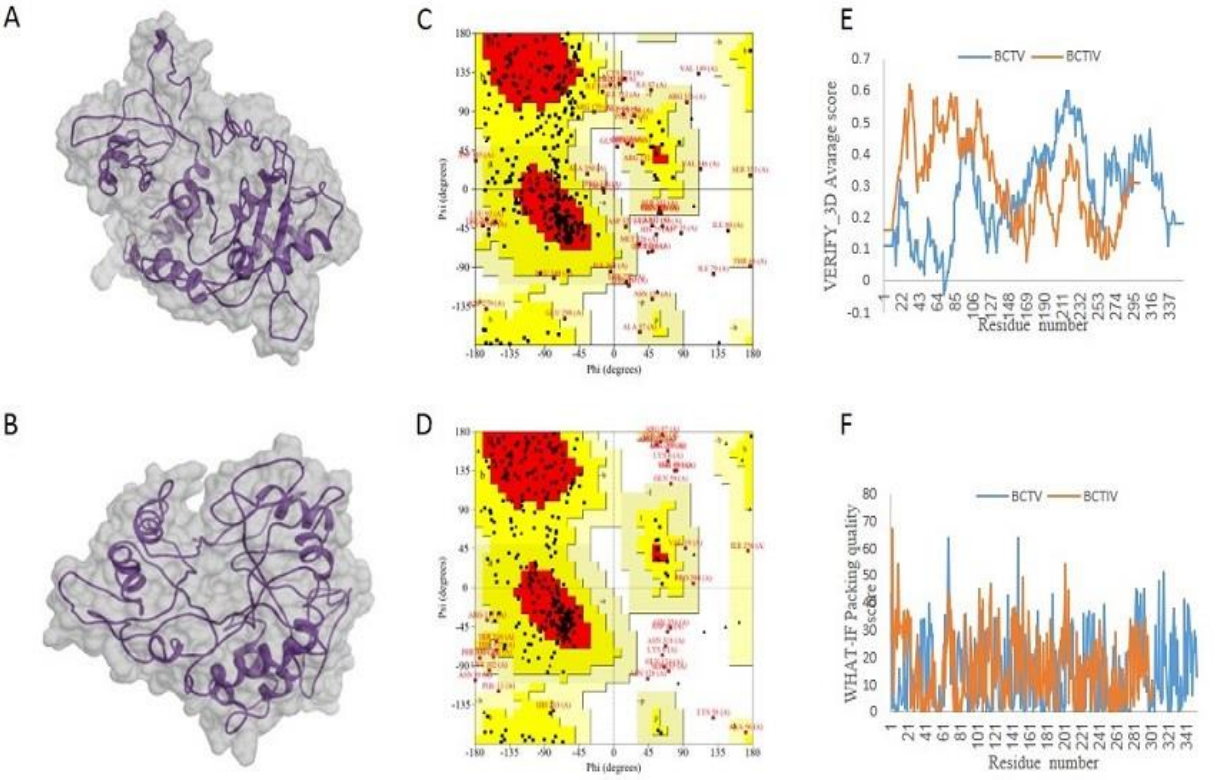

Figure 3 Ribbon representation of the structural models of Rep proteins from BCTIV (**A**) and BCTV (**B**). Validation of the structural models of Rep proteins from BCTIV(**C**) and BCTV (**D**) calculated by Ramachandran plot of PROCHECK, VERIFY_3D score (**E**), and WHAT-IF packing quality scores (**F**).

[DOR: 20.1001.1.22519041.2022.11.2.10.3]

Tertiary structures of Rep proteins of both viruses were predicted using I-TASSER (Zhang, 2008) and the best models obtained were further selected based on the indexes listed in Table 2, including the C-score, TM-score, RMSD, PROSA Z-score, PROCHECK, VERIFY_3D and ERRAT scores. Moreover, the validation parameters, i. e. Ramachandran plot, VERIFY_ 3D score, and WHAT-IF packing quality score, are summarized in Fig. 3.

Binding affinity of Rep proteins toward the nonanucleotide motifs of IBCTVs

The analysis of the interaction energy between BCTIV and BCTV Rep proteins and their nonanucleotide motifs showed that the highest total binding energy occurred between the BCTIV Rep and its nonanucleotide motif (-320.94), followed by that between the BCTV Rep and its nonanucleotide motif (-349.65) (Table 3). This indicated a relatively lower affinity of BCTIV Rep towards its cognate nonanucleotide motif compared to the BCTV complex, possibly justifying the higher titers of BCTV accumulating during single infections compared to BCTIV (Majidi *et al*., 2017).

Interestingly, when non-cognate interactions were considered, BCTIV Rep showed the lowest total binding energy score towards the nonanucleotide motif of BCTV (-502.69), while BCTV Rep had a score of -447.26 towards the BCTIV nonanucleotide motif. Since binding of the Rep proteins to the nonanucleotide motif is considered species-specific (Behjatnia *et al*., 1998), a higher affinity of a Rep towards a non-cognate nonanucleotide motif could lead to repressing the replication of the non-cognate virus through the inhibition of homologous Rep-nonanucleotide binding. In other terms, the higher affinity of BCTIV Rep for the nonanucleotide motif of BCTV could justify the relative decrease of the BCTV titer during mixed infections.

To further investigate the interactions between Reps and nonanucleotides, three-dimensional structures of the interactions between Rep proteins and the nonanucleotide motifs were obtained with HADDOCK and with the CHIMERA software (Fig. 4A). Hydrogen bonding and van der Waals interactions between nonanucleotide motifs and amino acid residues of Rep proteins which they were in interaction with nonanucleotides directly, were estimated by PDBsum server (Fig. 4B). This analysis showed that hydrogen bonds were more frequent in the interaction between the amino acid residues of BCTIV Rep with the nonanucleotide motif of BCTV (Fig. 4B). Moreover, complexes involving BCTIV Rep contained more hydrogen bond contacts than BCTV Rep. Arg 9, Lys 115, Arg 139, Arg 192 and Lys 223 are the most frequent amino acid residues of Rep proteins involved in binding nonanucleotide motifs.

Table 3 Statistics of HADDOCK results for top-ranked clusters of interactions between Rep proteins and their nonanucleotide motifs.

Interaction	Cluster rank	Haddock score	Cluster size	RMSD	Z-score	Energy (Kcal.mol^{-1})				Buried surface area (Å^2)
						Van der Waals	Electrostatic	Desolvation	Total	
BCTIV-BCTIV	8	-142.8	4	14.5	-1.8	-62.94	-258.00	-40.5	-320.94	1886.12
BCTIV-BCTV	2	-138.8	11	10.2	-1.2	-44.19	-458.49	-47.5	-502.69	1465.97
BCTV-BVTIV	2	-148.5	9	1.1	-2.2	-52.61	-394.64	-31.6	-447.26	1307.19
BCTV-BCTV	4	-130.1	7	7.6	-1.9	-53.62	-296.03	-23.1	-349.65	1210.35

[DOR: 20.1001.1.22519041.2022.11.2.10.3]

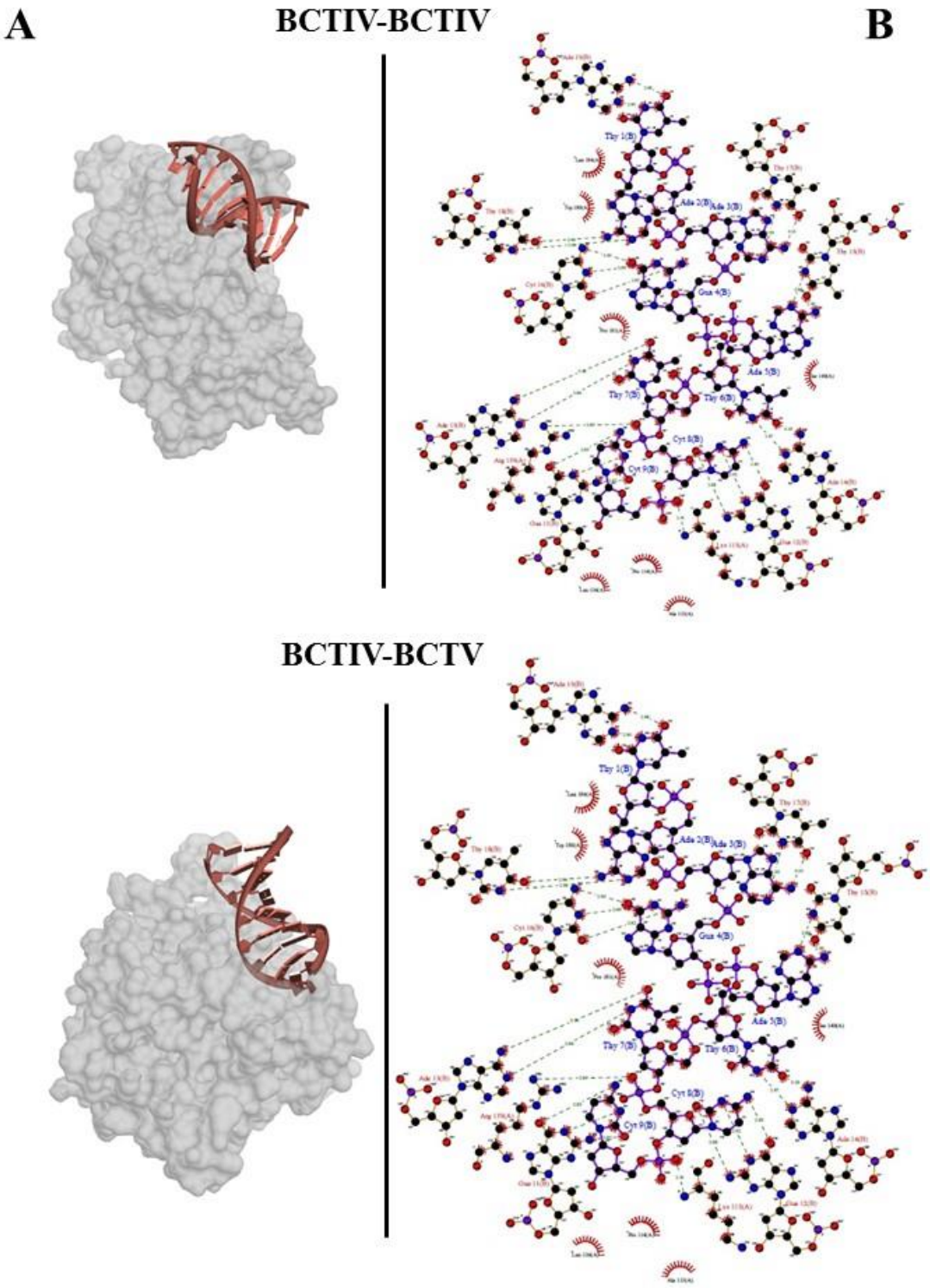

[DOR: 20.1001.1.22519041.2022.11.2.10.3]

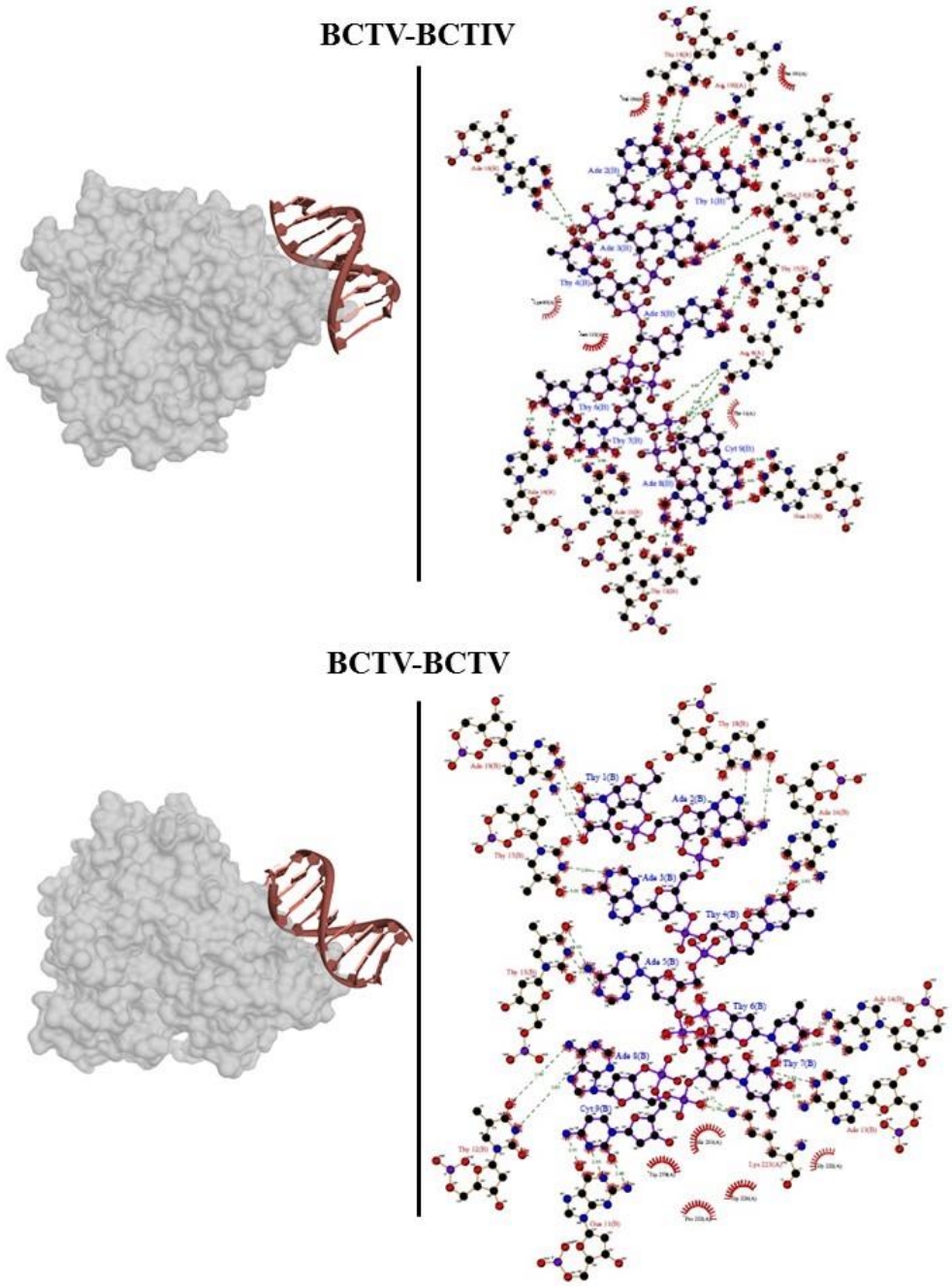

Figure 4 Rep/nonanucleotide interaction models. **A.** Superimposed view of the binding complex between the Rep proteins and the nonanucleotide motifs obtained with HADDOCK and CHIMERA software. The nonanucleotide and the Rep proteins have been represented as the red ribbon and the gray solid, respectively. **B.** Schematic view of the hydrogen bond interactions and nonbonded contacts between the nonanucleotide motifs and the residues involved in the protein binding sites obtained with the PDBsum server. Hydrogen bonding (dashed lines) and van der Waals interactions (spokes) are indicated. The surface is colored according to atom type, where carbon is black, nitrogen is blue, oxygen is red, and sulfur is yellow.
*In each complex, the first name referes to the Rep encoding virus and the second referes to the virus derided nonanucleotide motif.

[DOR: 20.1001.1.22519041.2022.11.2.10.3]

Discussion

Beet curly top Iran virus and Beet curly top virus are responsible for the curly top disease in sugar beet and some other dicot plants in Iran (Anabestani *et al*., 2016; Gharouni Kardani *et al*., 2013). Following isolation and sequencing of different complete genome sequences, relatively lower levels of nucleotide and amino acid sequence identities were determined between Iranian isolates of BCTIV and BCTV (Yazdi *et al*., 2008; Bozorgi *et al*., 2017). Since the newly described isolates shared < 77% sequence identity with members of the *Curtovirus* genus, a different classification and the new *Becurtovirus* genus was proposed (Varsani *et al*., 2014). The International Committee on Taxonomy of Viruses (ICTV) approved the new Becurtovirus genus that includes, besides BCTIV, *Spinach curly top Arizona virus* (SpCTAV) and *Exomis microphylla latent virus* (EMLV) (Zerbini *et al*., 2017).

The prevalence of BCTIV and BCTV varies in different fields. BCTIV has a higher incidence of infection in sugar beet fields, while other crops such as tomato, pepper, and bean were more frequently infected by BCTV (Anabestani *et al*., 2016). In terms of host range and symptom severity, BCTV has a wider host range and causes more severe symptoms than BCTIV (Anabestani *et al*., 2016). Nevertheless, during mixed infections by both viruses, increased disease symptoms occur compared to plants infected by individual viruses and this is accompanied by a higher accumulation of BCTIV DNA at the expense of BCTV (Majidi *et al*., 2017), suggesting that BCTIV interferes with the replication or the spread of BCTV (Majidi *et al*., 2017).

Among the factors responsible for the interference between viruses is the suppression of gene silencing, which could be exerted by one or both interacting viruses (Syller, 2012). For example, the helper-component proteinase (HC-Pro) of *Sweet potato feathery mottle virus* (SPFMV), a member of the genus *Potyvirus*, was shown to facilitate the systemic spread of *Potato virus X* (PVX) in *Ipomoea nil*, suggesting that this protein acted as a gene silencing suppressor, enhancing the long-distance movement of PVX in this host (Pruss *et al*., 1997; Sonda *et al*., 2000). Although different proteins of geminiviruses have been reported to have a silencing suppression activity (Fondong, 2013), the function of BCTIV encoded proteins during single- and mixed infections needs to be determined, and no information is available about silencing suppression activity.

Considering other factors potentially involved in the competitive interaction between BCTIV and BCTV, in the present work, we studied the distinct genomic characteristics of IBCTVs, focusing on the ability of Rep to interact with the nonanucleotide motif, a critical step during genome replication through the nuclease/ligase activity of Rep. For this, we predicted the structures of BCTIV and BCTV Rep proteins and evaluated by *in silico* studies their interactions with the nonanucleotide motifs of the two IBCTVs. Predictions of the primary, secondary, and tertiary structures of the Rep proteins of the Iranian isolates of BCTIV and BCTV were obtained using different bioinformatics tools. The sequence alignment studies revealed that the Rep sequences of the two IBCTVs have a low identity (23%), suggesting structural differences between them (Fig. 1). Moreover, the predicted secondary structures showed that random coils and α-helix were the most prevalent elements of the Rep proteins secondary structure, and β-strands were randomly distributed along the entire proteins (Fig. 2). The predicted 3D model of Rep proteins indicated significant differences between their tertiary structures, suggesting different interactions between protein-ligand (nonanucleotide motif) pairs (Fig. 3A). Moreover, physicochemical properties of Rep proteins showed a molecular weight of 41.86 kDa and 40.2 kDa, a pI of 6.83, an aliphatic index of 72.63 and 76.60, instability index of 54.73 and 36.77 for BCTIV and BCTV, respectively (Table 1). The isoelectric point is useful for the description of the acidic or basic character of a protein (Mukherjee and Mukhopadhyay, 2020). Here, theoretical pI data

[DOR: 20.1001.1.22519041.2022.11.2.10.3]

indicated the acidic nature of both Rep proteins. The instability index is generally used as an indicator of *in vivo* half-life of a protein. Proteins with an *in vivo* half-life lower than 5 h generally have an instability index higher than 40, while those with a half-life greater than 16 h have an instability index below 40 (Idicula-Thomas and Balaji, 2005). Here, the instability index calculated for BCTIV Rep was higher than that of BCTV Rep (Table 1), theoretically suggesting a longer half-life for the Rep of BCTV. The GRAVY index (the sum of hydropathic values of all amino acids divided by the protein length) is currently used to classify proteins in terms of hydrophobic (positive values) or hydrophilic (negative values) residues, while taking into account the length of the sequence of amino acids (Rodriguez-Ruiz *et al*., 2019). The results showed a similar GRAVY value for both Rep proteins.

All geminivirus genomes are characterized by a typical hairpin structure at the origin of virion-strand replication, consisting of a GC-rich stem and a loop containing a highly conserved AT-rich nonanucleotide motif, usually TAATATTAC (Zerbini *et al*., 2017). BCTIV has two nucleotide substitutions at positions 4 (G to T) and 8 (C to A) of this sequence motif (Varsani *et al*., 2014). Since the highly specific binding of Rep to this motif is crucial for the initiation of viral DNA replication through the rolling circle replication (RCR) mechanism (Behjatnia *et al*., 1998), we investigated the binding affinity of predicted structures of Rep proteins using molecular docking simulation studies to elucidate the parameters involved in the interaction of Rep proteins with the nonanucleotide motifs. The HADDOCK program was used to assess the binding affinity of the predicted Rep structures to their cognate and non-cognate ligands. Interestingly, the analysis of total binding energy, which mainly includes the contributions from electrostatic interactions, van der Waals interactions and desolvation effects in different Rep/nonanucleotide motif complexes, revealed that the interaction between BCTIV encoded Rep and the nonanucleotide motif of BCTV was the most stable complex (Table 3). This strong affinity is expected to influence the ability of BCTV Rep to interact with its cognate DNA. Accordingly, these results suggest that BCTIV Rep probably binds with more affinity to the functional site of BCTV Rep, making the site unavailable for interaction with the cognate Rep, preventing and/or reducing the interaction of BCTV Rep with the target motif. This finding can explain the reduced levels of replication and virus accumulation of BCTV during mixed infection with BCTIV (Majidi *et al*., 2017).

Finally, this *in silico* study provides an insight into the molecular interactions possibly involved in the interference between the two IBCTVs, opening a new horizon to elucidate the roles and interactions of different factors during mixed virus infections. Nonetheless, the effect of such interactions must be confirmed by *in vitro* or *in vivo* analysis of viral replication.

Conflicts of Interest: The authors declare no conflict of interest.

Author contributions: Saeid Tabein and Seyed Ali Hemmati conceived and designed the experiments, Seyed Ali Hemmati analyzed the data. Saeid Tabein, and Seyed Ali Hemmati wrote the paper.

Acknowledgments

Special thanks to Dr. Emanuela Noris from Institute for Sustainable Plant Protection, National Research Council, Torino, Italy, for her valuable editorial comments and helpful revision to improve the manuscript. This research was financially supported by Shahid Chamran University of Ahvaz, Ahvaz, Iran (Grant No.SCU.AP1400.38686).

References

Al-Khayyat, M. Z. S. and Al-Dabbagh, A. G. A. 2016. *In silico* Prediction and Docking of Tertiary Structure of LuxI, an Inducer Synthase of *Vibrio fischeri*. Reports of Biochemistry & Molecualr Biology, 4(2): 66-75.

[DOR: 20.1001.1.22519041.2022.11.2.10.3]

Altschul, S. F., Madden, T. L., Schaffer, A. A., Zhang, J., Zhang, Z., Miller, W. and Lipman, D. J. 1997. Gapped BLAST and PSI-BLAST: a new generation of protein database search programs. Nucleic Acids Research, 25(1): 3398-3402.

Anabestani, A., Behjatnia, S. A. A., Izadpanah, K., Tabein, S. and Accotto, G. P. 2017. Seed transmission of Beet curly top virus and Beet curly top Iran virus in a local cultivar of petunia in Iran. Viruses, 9: 299-311.

Anabestani, A., Izadpanah, K., Tabein S., Hamzeh-Zarghani, H. and Behjatnia, S. A. A. 2016. Beet curly top viruses in Iran: Diversity and incidence in plants and geographical regions. Iranian Journal of Plant Pathology, 51(4): 493-504.

Behjatnia, S. A. A., Dry, I. B. and Rezaian, M. A. 1998. Identification of the replication-associated protein binding domain within the intergenic region of tomato leaf curl geminivirus. Nucleic Acids Research, 26(4): 925-931.

Bolok Yazdi, H. R., Heydarnejad, J. and Massumi, H. 2008. Genome characterization and genetic diversity of beet curly top Iran virus: A geminivirus with a novel nonanucleotide. Virus Genes, 36(3): 539-545.

Bozorgi, N., Heydarnejad, J., Kamali, M. and Massumi, H. 2017. Splicing features in the expression of the complementary-sense genes of *Beet curly top Iran virus*. Virus Genes, 53(2): 323-327.

Colovos, C. and Yeates, T. O. 1993. Verification of protein structures: patterns of nonbonded atomic interactions. Protein Science, 2(9): 1511-1519.

de Beer, T. A. P., Berka, K., Thornton, J. M. and Laskowski, R. A. 2014. PDBsum additions. Nucleic Acids Research, 42: 292-296.

de Vries, S. J., van Dijk, M., and Bonvin, A. M. J. 2010. The HADDOCK web server for data-driven biomolecular docking. Nature Protocols, 5: 883-897.

Fondong, V. N. 2013. Geminivirus protein structure and function. Molecular Plant Pathology, 14(6): 635-649.

Gharouni Kardani, S., Heydarnejad, J., Zakiaghl, M., Mehrvar, M. Kraberger, S. and Varsani, A. 2013. Diversity of Beet curly top Iran virus isolated from different hosts in Iran. Virus Genes, 46(3): 571-575.

Heydarnejad, J., Keyvani, N., Razavinejad, S., Massumi, H. and Varsani, A. 2013. Fulfilling Koch's postulates for beet curly top Iran virus and proposal for consideration of new genus in the family *Geminiviridae*. Archives of Virology, 158(2): 435-443.

Idicula-Thomas, S., and Balaji, P. V. 2005. Understanding the relationship between the primary structure of proteins and its propensity to be soluble on overexpression in *Escherichia coli*. Protein Science, 14(3): 582-592.

Jeske, H., Lütgemeier, M. and Preiss, W. 2001. DNA forms indicate rolling circle and recombination-dependent replication of *Abutilon mosaic virus*. The EMBO Journal 20(21): 6158-6167.

Kurkcuoglu, Z., Koukos, P. I., Citro, N., Trellet, M. E., Rodrigues, J. P. G. L. M., Moreira, I. S., Roel-Touris, J., Melquiond, A. S., Geng, C., Schaarschmidt, J. and Xue, L. C. 2018. Performance of HADDOCK and a simple contact-based protein–ligand binding affinity predictor in the D3R Grand Challenge 2. Journal of Computer-Aided Molecular Design, 32(1): 175-185.

Majidi, A., Hamzehzarghani, H., Izadpanah, K. and Behjatnia, S. A. A. 2017. Interaction between Beet curly top Iran virus and the sever isolate of Beet curly top virus in three selective sugar beet cultivars. Journal of Plant Pathology, 99(2): 381-389.

Mukherjee, T. and Mukhopadhyay S. K. 2020. Comparative analysis of structural and functional aspects of phytoene synthase from *Meiothermus taiwanensis* strain RP. Annals of Microbiology, 70. Available from: doi.org/10.1186/s13213-020-01558-9.

Pawlowski, M., Gajda, M. J., Matlak, R. and Bujnicki, J. 2008. MetaMQAP: A meta-server for the quality assessment of protein models. BMC Bioinformatics, 9: 403. Available from: doi:10.1186/1471-2105-9-403.

[DOR: 20.1001.1.22519041.2022.11.2.10.3]

Pettersen, E. F., Goddard T. D., Huang, C. C., Couch, G. S., Greenblat, D. M., Meng, E, C. and Ferrin, T. E. 2004. UCSF Chimera--a visualization system for exploratory research and analysis. Journal of Computational Chemistry, 25(13): 1605-1612.

Pruss, G., Ge, X., Shi, X. M., Carrington, J. C., and Bowman Vance, V. 1997. Plant viral synergism: the potyviral genome encodes a broad-range pathogenicity enhancer that transactivates replication of heterologous viruses. The Plant Cell, 9(6): 859-868.

Rodriguez-Ruiz, H. A., Garibay-Cerdenares, O. L., Illades-Aguiar, B., Montano S., Jiang, X. and Leyva-Vazquez, M. A. 2019. *In silico* prediction of structural changes in human papillomavirus type 16 (HPV16) E6 oncoprotein and its variants. BMC Molecular and Cell Biology, 20(1): 35-46.

Soleimani, R., Matic, S., Taheri, H., Behjatnia, S. A. A., Vecchiati, M., Izadpanah K. and Accotto, G. P. 2013. The unconventional geminivirus Beet curly top Iran virus: Satisfying Koch's postulates and determining vector and host range. Annals of Applied Biology, 162(2): 174-181.

Sonda, S., Koiwa, H., Kanda, K., Kato, H., Shimono, M. and Nishiguchi, M. 2000. The Helper Component-Proteinase of Sweet potato feathery mottle virus Facilitates Systemic Spread of Potato virus X in *Ipomoea nil*. Phytopathology, 90(9): 944-950.

Syller, J. 2012. Facilitative and antagonistic interactions between plant viruses in mixed infections. Molecular Plant Pathology, 13(2): 204-216.

Taheri, H., Izadpanah, K. and Behjatnia S. A. A. 2012. *Circulifer haematoceps*, the vector of the Beet curly top Iran virus. Iranian Journal of Plant Pathology, 48(1): 48-45.

Thompson, J. D., Higgins, D. G. and Gibson, T. J. 1994. CLUSTAL W: improving the sensitivity of progressive multiple sequence alignment through sequence weighting, position-specific gap penalties and weight matrix choice. Nucleic Acids Research, 22(22): 4673-4680.

Varsani, A., Martin, D. P., Navas-Castillo, J., Moriones, E., Hernandez-Zepeda, C., Idris, A., Zerbini, F. Z. and Brown J. K. 2014. Revisiting the classification of curtoviruses based on genome-wide pairwise identity. Archives of Virology, 159: 1873-1882.

Zerbini, F. M., Briddon, R. W., Idris A., Martin, D. P., Moriones, E., Navas-Castillo, J., Rivera-Bustamante, R., Roumagnac, P. and Varsani A. 2017. ICTV virus taxonomy profile: *Geminiviridae*. Journal of General Virology, 98(2): 131-133.

Zhang, Y. 2008. I-TASSER server for protein 3D structure predictions. BMC Bioinformatics, 9: 40. doi.org/10.1186/1471-2105-9-40.

[DOR: 20.1001.1.22519041.2022.11.2.10.3]

تداخل بین ویروس ایرانی پیچیدگی بوته چغندرقند و ویروس پیچیدگی بوته چغندرقند: تخمینی درون رایانه‌ای از نقش برهمکنش بین پروتئین رِپ و موتیف نونانوکلئوتید

سعید تابعین* و سیدعلی همتی

گروه گیاه‌پزشکی، دانشکده کشاورزی، دانشگاه شهید چمران اهواز، اهواز، ایران.
پست الکترونیکی نویسنده مسئول مکاتبه: s.tabein@scu.ac.ir
دریافت: ۲۹ فروردین ۱۴۰۱؛ پذیرش: ۱۰ شهریور ۱۴۰۱

چکیده: ویروس ایرانی پیچیدگی بوته چغندرقند (BCTIV) و ویروس پیچیدگی بوته چغندرقند (BCTV)، عوامل ایجادکننده بیماری پیچیدگی بوته در چغندرقند و بسیاری دیگر از گیاهان دو لپه‌ای هستند. آلودگی مخلوط هر دو ویروس در بوته‌های چغندرقند باعث ایجاد برهمکنش هم‌افزایی می‌گردد که با علایم شدیدتر در مقایسه با بوته‌هایی که تنها با یک ویروس آلوده شده‌اند، همراه است. این برهمکنش، به‌ترتیب با افزایش و کاهش تیتر BCTIV و BCTV در آلودگی مخلوط همراه است. برهمکنش پروتئین همراه با همانندسازی (رِپ) با موتیف نونانوکلئوتید مستقر در مبدأ شروع همانندسازی، عاملی کلیدی در همانندسازی ژنوم جمینی‌ویروس‌ها است. در این مطالعه با استفاده از یک رویکرد درون رایانه‌ای، دخالت احتمالی برهمکنش بین پروتئین‌های رِپ و موتیف‌های نونانوکلئوتید در تداخل بین BCTIV و BCTV به‌هنگام آلودگی‌های مخلوط مورد ارزیابی قرار گرفت. تعیین ویژگی‌های فیزیکوشیمیایی پروتئین رِپ هر دو ویروس با استفاده از ابزار SOMPA انجام شد و ساختارهای درجه دوم و سوم آن‌ها با استفاده از سرورِ I-TASSER تخمین زده شد. پس از آن، تمایل اتصال هر پروتئین رِپ به موتیف‌های نونانوکلئوتید خودی و ناخودی با استفاده از شبیه‌سازی‌های Docking مورد ارزیابی قرار گرفت. آنالیز خوشه‌ای HADDOCK نشان داد که انرژی کل اتصال پروتئین رِپ BCTV به موتیف نونانوکلئوتید خودی همین‌گونه، کم‌تر از کمپلکس ایجاد شده توسط گونه BCTIV است. به‌طرز جالب‌توجهی، پروتئین رِپ BCTIV بالاترین تمایل اتصال را به موتیف نونانوکلئوتید BCTV نشان داد. از آنجایی‌که همانندسازی جمینی‌ویروس‌ها به برهمکنش‌ها و فعالیت‌های اختصاصی گونه پروتئین رِپ بستگی دارد، نتیجه به‌دست آمده می‌تواند به‌عنوان عامل تداخل رقابتی BCTIV در برابر BCTV در نظر گرفته شود.

واژگان کلیدی: ویروس‌های پیچیدگی بوته چغندرقند، آلودگی‌های مخلوط، موتیف‌های نونانوکلئوتید، رِپ، شبیه‌سازی Docking

[DOR: 20.1001.1.22519041.2022.11.2.10.3]